Synthesis of Few-Layer GaSe Nanosheets for High Performance Photodetectors

PingAn Hu,[†,*] Zhenzhong Wen,[†] Lifeng Wang,[†] Pingheng Tan,[‡] and Kai Xiao[§,*]

[†]Key Lab of Microsystem and Microstructure, Harbin Institute of Technology, Ministry of Education, No. 2 YiKuang Street, Harbin, 150080, P.R. China, [‡]State Key Laboratory for Superlattices and Microstructures, Institute of Semiconductors, Chinese Academy of Sciences, Beijing 100083, China, and [§]Center for Nanophase Materials Sciences, Oak Ridge National Laboratory, One Bethel Valley Road, Oak Ridge, Tennessee 37831, United States

ABSTRACT

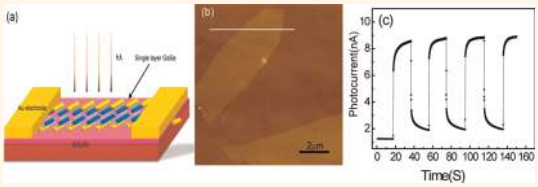

Two-dimensional (2D) semiconductor nanomaterials hold great promises for future electronics and optics. In this paper, a 2D nanosheets of ultrathin GaSe has been prepared by using mechanical cleavage and solvent exfoliation method. Single- and few-layer GaSe nanosheets are exfoliated on an SiO_2/Si substrate and characterized by atomic force microscopy and Raman spectroscopy. Ultrathin GaSe-based photodetector shows a fast response of 0.02 s, high responsivity of 2.8 AW^{-1} and high external quantum efficiency of 1367% at 254 nm, indicating that the two-dimensional nanostructure of GaSe is a new promising material for high performance photodetectors.

KEYWORDS: gallium selenide · nanosheets · photodetectors

A photodetector is a sensor of light or other electromagnetic radiation, which can convert incident radiation into an electrical signal. Photodetectors are applied in wide fields of space communication and chemical/biological detection.[1−5] The current intense interest in the exploitation of nanostructures in photodetectors is mainly attributable to two reasons: first, large surface-to-volume ratio and small dimensions of nanostructured materials can yield higher light sensitivity than their bulk counterparts, and the photocarrier lifetime is considerably prolonged due to charge separation promoted by surface states;[6−8] second, the bandgap of nanomaterials strongly depends on their sizes and this size effect permits the spectral tunability within a single material system, enabling multispectral photodetectors that are sensitive in the visible, near-infrared, and ultraviolet.[9,10] Quantum dots and one-dimensional (1D) nanostructures of carbon nanotubes, semiconducting nanowires, and nanobelts have been utilized to develop high performance photodetectors. For example, infrared photodetectors with a large photocurrent gain (>$10^3$$AW^{-1}$) and a high sensitivity were fabricated from PbS colloidal quantum dots (QDs) *via* solution processing;[10] high performance photodectors have been demonstrated by using 1D semiconducting nanostructures of ZrS, CdS, ZnSe, *etc*.[11−14] One obstacle for nanoscale photonics in real application is the complexity in manipulation and fabrication of QDs or 1D nanostructures. Therefore, there is still a necessity for exploration of new optical nanostructures that can possess characteristics of both high performance photocurrent properties and practicality in manufacture.

Two dimensional (2D) nanostructures are currently becoming the focus of nanoscience. Graphene, which has a linear energy dispersion relation (vanishing effective mass), and an extremely high mobility (approaching *ca.* 200000 cm^2 V^{-1} s^{-1} for a free sheet) of both electrons and holes,[15,16] is the most widely studied 2D nanomaterial. These properties render graphene potential in fast electronics and research models of physics. Inspired by the discovery of graphene, research has been triggered in other 2D inorganic materials such as transition metal dichalcogenides (MoS_2, WS_2 *etc.*), transition metal oxides, and other 2D compounds (*e.g.*, BN, Bi_2Te_3, and Bi_2Se_3).[17,18] These single layer or few layer inorganic graphene analogues can be produced by mechanical cleavage, chemical exfoliation, or self-assembly.[19,20] Compared to quantum dots and one-dimensional nanostructure of nanowires and carbon nanotubes, 2D materials are more compatible with present microfabrication techniques, and are easily fabricated into complex structures. To the best of our knowledge, so far, there are few reports regarding photodetectors made of 2D semiconductor nanomaterials,[21,22] although zero bandgap,

* Address correspondence to hupa@hit.edu.cn, xiaok@ornl.gov.

Received for review February 28, 2012 and accepted June 4, 2012.

Published online June 07, 2012
10.1021/nn300889c

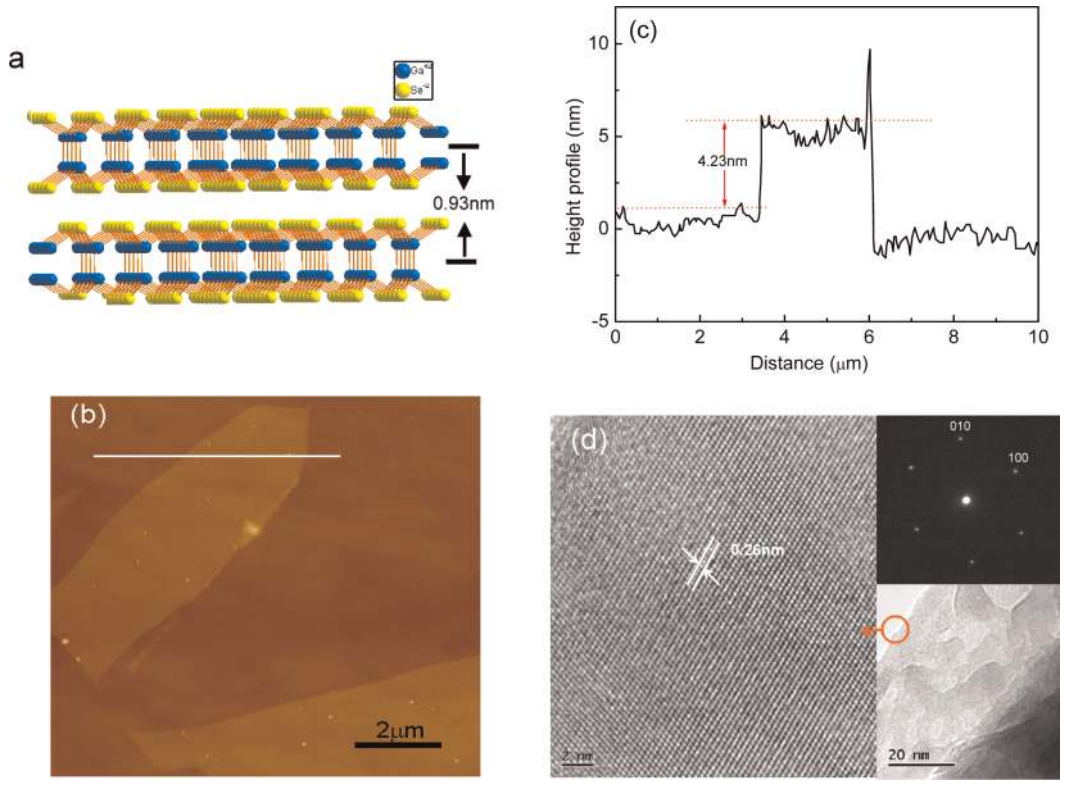

Figure 1. Characterization of as-prepared few-layer GaSe: (a) three dimensional structure of GaSe, single layers, 9.3 Å thick; (b) AFM imaging of a few-layer GaSe flake on a silicon substrate with a 300 nm thick oxide layer; (c) cross-sectional plot along the line in b determines the thickness to be 4.23 nm; (d) high resolution TEM image with inserted selected area electron diffraction pattern.

single layer, or few layer graphene transistors have been utilized as novel fast photodetectors, in which electron−hole pairs are separated to produce photocurrent by exploiting external electrical fields.[23] In this communication, we demonstrate the preparation and characterization of few-layer gallium selenide (GaSe) nanomaterials; further, we first demonstrate their photodetector devices.

GaSe is a typical example of layered materials from the transitionmetal chalcogenide family. GaSe crystals are composed of vertically stacked Se−Ga−Ga−Se sheets held together by weak forces such as van der Waals with some ionic or Coulomb contributions (shown in Figure 1a).[24] They are usually p-type semiconductors with an indirect bandgap of 2.11 eV, which is only 25 meV lower than the direct bandgap.[24−26] However, the difference between direct and indirect band edges is so small that electrons can easily be transferred between this minimum with a small amount of thermal energy. GaSe quantum dots and nanowires show a distinct influence of quantum confinement on their electronical and optical properties.[27,28] Other features of GaSe that render it promising for nanophotonic device applications include the absence of dangling bonds and thermal stability up to 600 °C.

RESULTS AND DISCUSSION

The ultrathin GaSe flakes prepared by mechanical exfoliation are characterized by using atomic force microscopy (AFM) and transmission electron microscopy (TEM). Figure 1a shows the schematic structure of single layer GaSe which has a thickness of 0.93 nm. The thickness of GaSe flakes is mainly in the range of 1−8 nm, which corresponds to a layer number of 1−8. For instance, a typical GaSe flake lying on SiO_2/Si was determined to be ∼4 nm thick by AFM measurement, indicating ∼4 layers of GaSe (shown in Figure 1b,c). The GaSe flakes are further characterized by using TEM (Figure 1d,e). The lattice fringes show that the GaSe flakes have good crystal quality, and the observed *d* spacings correspond to the (110) plane of GaSe.[29] The selected area electron diffraction (SAED) pattern (Figure 1d) is also consistent with the simulated layer structure of GaSe. To further characterize the flakes, their chemical compositions are measured by energy-dispersive X-ray spectroscopy (EDS) (Supporting Information, Figure S1), confirming that the flakes have a Ga/Se stoichiometric ratio of ∼1:1.

Raman spectra on as-prepared ultrathin GaSe flakes, as well as bulk crystals, were collected for comparisons. As shown in Figure 2, Raman spectra were collected for mechanically exfoliated thin flakes and bulk crystal on SiO_2 substrate. A_{1g} indicates planar vibration, and E_{1g}, E_{2g} associate with the vibration of selenides in the out-of-plan direction. Six Raman active modes of A_{1g}, E_{2g}, and E_{1g} symmetry are found in Figure 2, which correspond well with the literature.[30,31] Two A_{1g} modes are

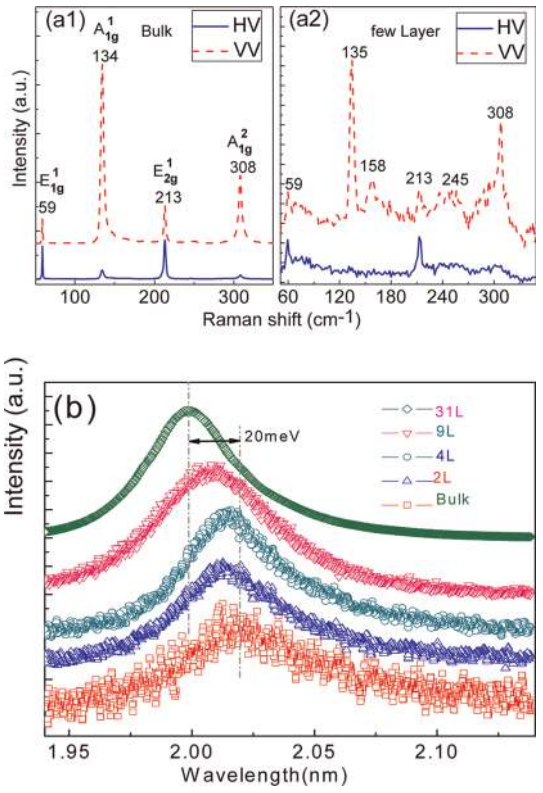

Figure 2. (a) Raman spectra taken from bulk GaSe crystal and few layer GaSe flakes where HV and VV configurations denote that the incident light is perpendicular or parallel to the scattered light; (b) layer number dependent photoluminescent spectra of GaSe flake and bulk GaSe crystal.

observed at 134 and 308 cm^{-1}. The Raman peak at 213 cm^{-1} comes from the E_{2g} mode, and another E_{2g} mode that should appear at 19 cm^{-1} is beyond the detection limit of the Raman system because of its low frequency. One E_{1g} mode appears at 59 cm^{-1}, while another one at 249 cm^{-1} is very weak. When polarized Raman scattering is performed with the incident laser normal to the base plane of bulk GaSe, the E_{1g} and E_{2g} modes at 59 and 213 cm^{-1} show the same intensity whether the incident light is parallel (VV) or perpendicular (HV) to the scattered light. However, the two A_{1g} modes are very strong in the VV polarization configuration but are very weak in the HV polarization configuration. For few-layer GaSe flakes, a significant decrease in thickness can significantly weaken the intensity of Raman vibrations, as can be seen from the signal-to-noise of the Raman spectra of few layer GaSe flakes shown in Figure 2a2. The polarization and peak position of each mode in few-layer GaSe are similar to that in bulk GaSe, indicating good crystal structure.

PL emission from several few layered GaSe flakes was measured and shown in Figure 2b. The peak position shows a slight blueshift with a decrease in the layer number, in comparison to that of bulk GaSe. This blueshift has been observed in few MoS_2 layers,[32] known as another typical layered semiconductor. A blueshift of 20 meV is observed between 2 layer and bulk GaSe, which is smaller than the case of MoS_2. This blueshift is possibly due to the modification of bandgap structure caused by the thickness decrease of layered GaSe, differing from nonlayer semiconductor nanomaterials (*e.g.*, CdSe, CdS quantum dots) whose optical properties are strongly influenced by a quantum confinement effect. For example, the optical bandgap of an ultrathin MoS_2 flake was transformed from indirect bandgap to direct one with decreasing thickness, and the MoS_2 monolayer emits light more strongly than its bulk material.[31] Further theoretical calculations on band structure of few layered GaSe flakes will be performed to understand this result.

To measure the photoelectrical properties, a monochromatic light is vertically incident on a GaSe device, and the corresponding photoelectric behavior is recorded (as shown in Figure 3a). Figure 3b is an SEM image of a typical device. The influence of wavelength on the photoresponse is investigated (Figure 3c,d). Figure 3c shows the *I*–*V* curves of photodetectors illuminated with different wavelengths and under dark conditions. Figure 3d shows the wavelength dependent photocurrent at 5 V, which is calculated from Figure 3c. The photocurrents increase when the wavelength of light decreases from 610 to 254 nm. Especially, a significant increase in photocurrent is observed when the device is illuminated with short lights. This indicates that 2D GaSe-based photodetectors are highly sensitive to UV–visible light. The ray with a photon energy higher than the bandgap of 2D GaSe (~2 eV, wavelength < 620 nm) can produce hole–electron pairs in GaSe flake. A shorter excitation wavelength of light provides higher excitation energy which increases the photocurrent. As shown in Figure 3d, with the light irradiation of 254 nm on and off, the current in the devices showed two distinct states: a "low" current of ~1 nA in the dark at 1 V and a "high" current of 8.8 nA under illumination, giving an on/off switching ratio of ~8. The switching between these two states is very fast and reversible, allowing the device to act as a high quality photosensitive switch. The high photosensitivity of the GaSe devices is further confirmed by photocurrent measurements on the devices at different incident light intesities (as shown in Figure 3f). When the intensity of the incident light was changed, the photocurrent of the device changed accordingly. This GaSe nanosheet device can be proposed to be a simple metal-semiconductors-metal (MSM) structure consiting of two schottky barrier contacts connected back to back. Under an applied voltage, one of contacts is reverse biased (cathode) and the other contact is forward (anode), creating an electric field in the GaSe flake. Ultrathin GaSe can strongly absorb photons from the visible to the near-ultraviolet, and electron–hole pairs are generated.[31]

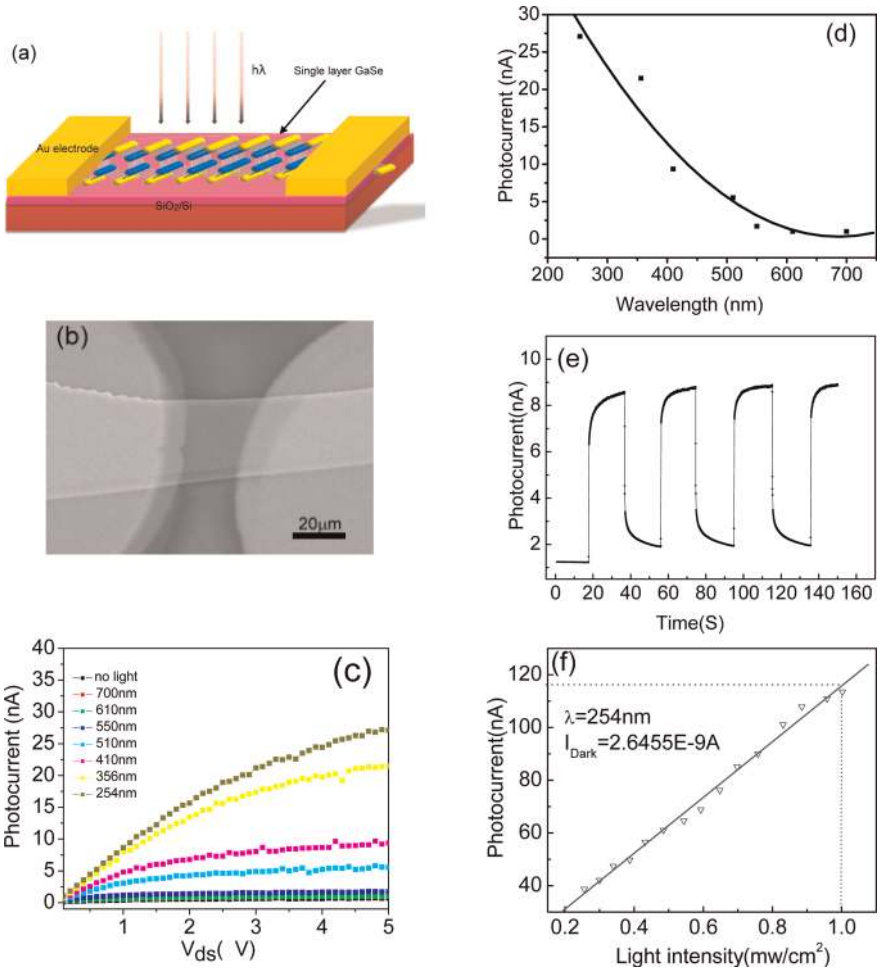

Figure 3. Characterization of few-layer GaSe photodetectors: (a) schematic drawing of the GaSe photodetectors; (b) SEM image of a typical device; (c) $I-V$ curves of photodetectors illuminated with different wavelengths; (d) wavelength-dependent photocurrent; (e) photocurrent as function of time at bias voltage of 1 V; (f) photocurrent as function of illumination density, LDR of the device under light irradiation of 254 nm. Inset is the dark current of the device. V_D = 2 V.

The pairs become separated by the electric field, and a photocurrent is generated.

The detector current responsivity (R_λ), defined as the photocurrent generated per unit power of the incident light on the effective area of a photoconductor, and the external quantum efficiency (EQE) defined as the number of electron−hole pairs excited by one absorbed photon, are critical parameters for a photodetector. R_λ and EQE can be expressed as $R_\lambda = \Delta I/PS$ and EQE = $hcR_\lambda/(e\lambda)$, where ΔI is the photoexcited current; P is the light power intensity irradiated on the GaSe; S is the effective area of photodetector; h is Planck's constant; e is electron charge; and λ is the excitation wavelength. From our experimental results, under an illumination of 254 nm at 5 v (calculated from Figure 2c), the R_λ and EQE are calculated to be ~2.8 AW^{-1} and ~1367%, respectively. The high R_λ and EQE are due to a high surface ratio which causes an efficient adsorption of photons. These performace parameters of ultrathin GaSe photodetectors can be comparable with those devices that are made of nanowire and nanotubes.[10−14] Although some nanoscale photodetectors have been demonstrated with nanowires or nanotubes in the past ten years,[10−14] their pratical application in high yield, scalable sytems faces formidable engineering in assembly and other aspects of manufacturing. Materials in 2D geometries can avoid these limitations since they are compatible with established device designs and processing approaches in the semiconductor industry. All of these results demonstrate that atomically thin GaSe can be used in highly sensitive nanoscale photodetectors and fast photoelectric switches.

An important photodetector feature of merit is the linear dynamic range (LDR) or photosensitivity linearity (typically quoted in dB). LDR is given by LDR = 20 log-(I_{ph}/I_{dark}), where I_{ph} is the photocurrent, measured at light intensity of 1 mW cm^{-2}. The LDR is calculated from Figure 3f: under illumination with visible light from a 500 W halogen lamp, the calculated LDR is 32.8 dB which is less than those of InGaAs photodetectors (66 dB).[33] These modest LDR values are limited by the relatively low ratio of photocurrent versus dark current, thus leaving room for future improvement.

Response time is another key factor for photodetector performance. A slow response time can limit their practical application. Response times for current rise and fall obtained from some 1D nanostructures or graphene oxide based photodetectors range from seconds to several tens of minutes.[10−14] This possibly results from a difference in the materials or devices structures. Figure 4 shows the time responses of photocurrent in the thin GaSe photodectors under an UV illumination of 254 nm as it is turned on or off. The dynamic response to the UV illumination for rise and fall in our devices can be expressed by: $I(t) = I_{dark} + A\exp(t/\tau)$ and $I(t) = I_{dark} + A\exp(-t/\tau)$, where I_{dark} is the dark current; A is a scaling constant; τ is a time constant; and t is the time when the UV is switched on or off. The time constant can be calculated by fitting the experimental data. The photocurrent of this device rises within 0.02 s under UV irradiation, and then increases by a little slower process of ~0.3 s saturation. The photocurrent starts a fast decay process, in which the current drops quickly for 0.037 s when the irradiation is turned off. The subsequent slow decay lasts 7 s before the current decreases reach the initial dark current. The time constant τ is calculated to be 0.0157 s according to the above equation and data in Figure 3. Adimittedly, this response time is much slower than that of tranditional metal−semiconductor−metal (MSM) photodetectors which have a typical switching time on the order of 10^{-6}−10^{-9} seconds. This slow response time is possibly caused by the interaction between the GaSe nanosheet and SiO_2 surface, because a large surface-to-volume ratio tends to induce defects and dangling bonds on the surface of GaSe. To explore the substrate surface effect on the photoresponse, a comparison experiment was performed: No photoresponse was observed when a light of 254 nm was illuminated on the Au-SiO_2/Si device without the GaSe nanosheet, which excludes the possible occurrence of photoresponse in SiO_2/Si. More investigation should be carried out to reveal the intrinsic reason of slow response. But the ultrathin GaSe based photodetectors here show a much faster response time compared to that of some of the reported nanostructure optics.[10−14]

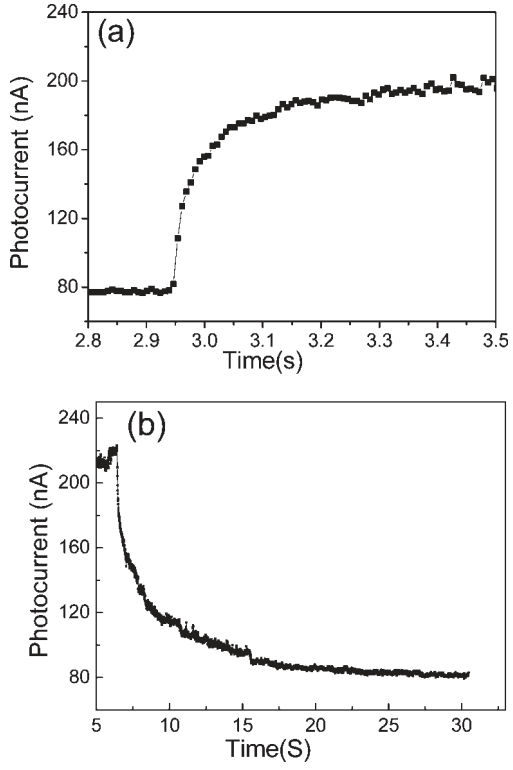

Figure 4. Time resolved response of photocurrent: (a) rise, (b) decay.

To demonstrate that the 2D nanostructure can enhance the performance of photodetectors, the photoresponse properties of bulk GaSe (length × width × thickness = 2 mm × 1 mm × 0.5 mm) was measured. The device configuration and photoresponse data including photocurrent *versus* power, photoswitching behavior is shown in the Supporting Information Figure S3. Under the illumination with 254 nm light (shown in Figure 3S), the ratio of photocurrent *versus* dark is around 0.38, the rise time is about 0.09 s. The R_λ and EQE are calculated to be 0.227 A/W and 110%. These performance parameters of photoresponse are much lower than those of GaSe nanosheet described above, proving that 2D nanostructure can improve the performance of photodetectors. Further, we compare the key performance parameter of our few-layer GaSe photodetectors to other reported 2D nanosheet optical devices, and the results are summarized in Table 1. GaSe nanosheet photodetectors show much higher responsivity and quantum efficient than the other reported 2D nanosheet devices,[21,22,31] and a faster response time than that of single layer MoS_2 photodetector.[21]

CONCLUSIONS

Atomically thin GaSe nanosheets, a new 2D semiconducting nanostructure, were prepared by exfoliation of the corresponding layered bulk crystals.

TABLE 1. Comparison of the Critical Parameters for the Reported 2D-Nanostructure Photodetectors

photodetectors	special responsivity (R_λ) [A W^{-1}]	quantum efficiency (QE) [%]	response time	ref
single layer MoS_2	7.5×10^{-3}		50 ms	21
graphene oxide	4×10^{-3}	0.3	2s	22
graphene	1×10^{-3}	6−16	~ps	31
few-layer GaSe	2.8	1367	20 ms	this work

The UV−visible photodetectors made by using atomically thin GaSe were characterized in terms of wavelength, power dependent photoresponse, and time-resolved photocurrent. The response time, responsivity, and external quantum efficiency of GaSe-nanosheet-based photodetectors are 0.02 s, 2.8 AW^{-1}, and 1367%, respectively. This demonstrates that the two-dimensional nanostructure of GaSe can be effectively used in high performance nanoscale photodetectors.

EXPERIMENTAL SECTION

The GaSe laminar precursor was obtained by a modified Bridgman method. The few layer GaSe nanoheets were made from a bulk layer precursor by a solvent or mechanical cleavage method. The thickness and layer number were determined by using atomic force microscopy (AFM). The composition and structure of few layer GaSe were characterized and analyzed by scanning electron microscopy (SEM, JSM-6301F), and transmission electron microscopy (TEM, JEOL-2010F) attached with an energy-dispersion X-ray spectroscopy (EDS). Raman and photoluminscence (PL) spectra were collected for bulk samples and nanosheets of GaSe using a Horiba-Jobin Yvon HR800 which is equipped with a liquid-nitrogen-cooled CCD. The laser excitation wavelength of 532 nm came from a diode pumped solid state laser with a typical excitation intensity of about 100 kW cm^{-2} to avoid sample heating. The Raman and PL measurements were done in a back-scatter geometry using a 100× objective lens (NA = 0.90) and a 600 or 1800 groove/mm grating (dependent on the spectral resolution) at room temperature. Polarized Raman scattering with the incident laser normal to the base plane of bulk GaSe was performed to identify the crystal oritation of bulk and few layer GaSe with the incident light parallel (VV) or perpendicular (HV) to the scattered light. The ultrathin GaSe was transferred to a silicon wafer with an oxidized layer of 300 nm. Cr/Au electrodes with 10 nm thick Cr and 100 nm thick Au were fabricated using a shadow mask. The devices with a gap of 20 μm were then annealed at 200 °C to reduce resistance. Photoelectric data are collected using a light source with a 500 W xenon lamp. Monochromatic wavelengths of 254−610 nm were obtained using optical filters. The photocurrent measurements were carried out using Lakeshore probe station and an HP 4140B semiconductor parameter analyzer. The intensities of incident beams were measured by a power and energy meter (model 372, Scienteck). The IR light was filtered throughout the experiments with a Toshiba IRA-25s filter (Japan) to protect the electrodes from heat.

Conflict of Interest: The authors declare no competing financial interest.

Acknowledgment. This work is supported by NSFC grants (61172001,10874177), special funds for the Major State Basic Research of China 2009CB929301, the Scientific Research Foundation for the Returned Overseas Chinese Scholars, State Education Ministry and the Fundamental Research Funds for Central Universities and Chinese Program for New Century Excellent Talents in University. Part of this research was conducted at the Center for Nanophase Materials Sciences, which is sponsored at Oak Ridge National Laboratory by the Scientific User Facilities Division, Office of Basic Energy Sciences, U.S. Department of Energy.

Supporting Information Available: The chemical composition of GaSe nanosheets is measured in Figure S1 by using EDS; (Figure S2) current versus time curve for the Au-SiO_2/ Si device without GaSe nanosheet under illumination; (Figure S3) (a) optical image, (b) light power, and (c) time dependent photoresponse of bulk GaSe devices. This material is available free of charge *via* the Internet at http://pubs.acs.org.

REFERENCES AND NOTES

1. Kolmakov, A.; Zhang, Y. X.; Cheng, G. S.; Moskovits, M. Detection of CO and O_2 Using Tin Oxide Nanowire Sensors. *Adv. Mater.* **2003**, *15*, 997–1000.
2. LaFratta, N.; Walt, D. R. Very High Density Sensing Arrays. *Chem. Rev.* **2008**, *108*, 614.
3. Lao, S.; Park, M. C.; Kuang, Q.; Deng, Y. L.; Sood, A. K.; Polla, D. L.; Wang, Z. L. Giant Enhancement in UV Response of ZnO Nanobelts by Polymer Surface-Functionalization *J. Am. Chem. Soc.* **2007**, *129*, 12096.
4. He, J. H.; Zhang, Y. Y.; Liu, J.; Moore, D.; Bao, G.; Wang, Z. L. ZnS/Silica Nanocable Field Effect Transistors as Biological and Chemical Nanosensors. *J. Phys. Chem. C.* **2007**, *111*, 12152.
5. Ji, S. L.; Ye, C. H. Single-Crystalline ZnS Nanobelts as Ultraviolet-Light Sensors. *J. Mater. Sci. Technol.* **2008**, *24*, 457.
6. Sun, Y. G.; Wang, H. H. Hydrothermally Grown Oriented ZnO Nanorod Arrays for Gas Sensing Applications. *Adv. Mater.* **2008**, *19*, 2818.
7. Li, L.; Fang, X. S.; Li, G. H. Bi-Based Nanowire and Nanojunction Arrays: Fabrication and Physical Properties. *J. Mater. Sci. Technol.* **2007**, *23*, 166.
8. Li, L.; Koshizaki, N.; Li, G. H. Nanotube Arrays in Porous Anodic Alumina Membranes. *J. Mater. Sci. Technol.* **2008**, *24*, 550.
9. Konstantatos, G. Sergeant, E. H. Nanostructured Materials for Photon Detection. *Nat. Nanotechnol.* **2010**, *5*, 391–400.
10. Howard, I.; Fischer, A.; Hoogland, S.; Clifford, J.; Klem, E.; Levina, L.; Sargent, E. H. Ultrasensitive Solution-Cast Quantum Dot Photodetectors. *Nature* **2006**, *442*, 180–183.
11. Fang, X. S.; Bando, Y.; Liao, M. Y.; Zhai, T. Y.; Gautam, U. K.; Li, L.; Koide, Y.; Golberg, D. An Efficient Way To Assemble ZnS Nanobelts as Ultraviolet-Light Sensors with Enhanced Photocurrent and Stability. *Adv. Funct. Mater.* **2010**, *20*, 500–508.
12. Li, L.; Fang, X. S.; Zhai, T. Y.; Liao, M. Y.; Gautam, U. K.; Wu, X. C.; Koide, Y.; Bando, Y.; Golberg, D. Electrical Transport and High-Performance Photoconductivity in Individual ZrS_2 Nanobelts. *Adv. Mater.* **2010**, *22*, 4151–4156.
13. Li, L.; Wu, P.; Fang, X. S.; Zhai, T. Y.; Dai, L.; Liao, M. Y.; Koide, Y.; Wang, H. Q.; Bando, Y.; Golberg, D. Single-Crystalline CdS Nanobelts for Excellent Field-Emitters and Ultrahigh Quantum-Efficiency Photodetectors. *Adv. Mater.* **2010**, *22*, 3161–3165.
14. Zhang, A.; Kim, H. K.; Cheng, J.; Yu., H. Ultrahigh Responsivity Visible and Infrared Detection Using Silicon Nanowire Phototransistors. *Nano Lett.* **2010**, *10*, 2117–2120.
15. Novoselov, K. S.; Geim, A. K.; Morozov, S. V.; Jiang, D.; Zhang, Y.; Dubonos, S. V.; Grigorieva, I. V.; Firsov, A. A. Electric Field Effect in Atomically Thin Carbon Films. *Science* **2004**, *306*, 666.
16. Geim, A. K.; Novoselov, K. S. Flexible Graphene Films *via* the Filtration of Water-Soluble Noncovalent Functionalized Graphene Sheets. *Nat. Mater.* **2007**, *6*, 183.
17. Coleman, J. N.; Lotya, M.; O'Neill, A.; Bergin, S. D.; King, P. J.; Khan, U.; Young, K.; Gaucher, A.; De, S.; Smith, R. J.; Shvets, I. V.; Arora, S. K.; *et al.* Two-Dimensional Nanosheets Produced by Liquid Exfoliation of Layered Materials. *Science* **2011**, *331*, 568.
18. Novoselov, K. S.; Jiang, D.; Schedin, F.; Booth, T. J.; Khotkevich, V. V.; Morozov, S. V.; Geim, A. K. Two-Dimensional Atomic Crystals. *Proc. Natl. Acad. Sci. U.S.A.* **2005**, *102*, 10451–10453.
19. Zhao, Y. M.; Hughes, R. W.; Su, Z. X.; Zhou, W. Z.; Gregory, D. H. Synthesis of Bismuth Telluride Nanosheets of a Few Quintuple Layers in Thickness. *Angew. Chem., Int. Ed.* **2011**, *50*, 10397–10401.

20. Ramakrishna Matte, H. S. S.; Gomathi, A.; Manna, A. K.; Late, D. J.; Datta, R. J.; Pati, S. K.; Rao, C. N. R. MoS_2 and WS_2 Analogues of Graphene. *Angew. Chem., Int. Ed.* **2010**, *49*, 4059–4062.
21. Yin, Z; Li., H; Li, H; Jiang, L.; Shi, Y.; Sun, Y.; Lu, G.; Zhang, Q.; Chen, X.; Zhang, H. Single Layer MoS_2 Photodetectors. *ACS Nano* **2012**, *6*, 74–80.
22. Chitara, B.; Panchakarla, L. S.; Krupanidhi, S. B.; Rao, C. N. R. Infrared Photodetectors Based on Reduced Graphene Oxide and Graphene Nanoribbons. *Adv. Mater.* **2011**, *23*, 5419–5423.
23. Thomas, M.; Xia, F.; Avouris, P. Graphene Photodetectors for High-Speed Optical Communications. *Nat. Photon.* **2010**, *4*, 297.
24. Wieting, T. J.; Schluter, M. Electrons and Phonons in Layered Crystal Structures. *The Netherlands*, **1979**, Vol. *3*.
25. Mooser, E.; Schluter, M. The Band-Gap Excitons in Gallium Selenide. *NuoVo Cimento* **1973**, *18B*, 164.
26. Capozzi, V. Optical Spectroscopy of Extrinsic Recombinations in Gallium Selenide. *Phys. Rev. B* **1989**, *40*, 3182.
27. Balitskii, A.; Borowiak-Palen, E.; Konicki, W. Synthesis and Characterization of Colloidal Gallium Selenide Nanowires. *Cryst. Res. Technol.* **2011**, *46*, 417–420.
28. Chikan, V.; Kelley, D. F. Synthesis of Highly Luminescent GaSe Nanoparticles. *Nano Lett.* **2002**, *2*, 141–145.
29. *Powder Diffraction Files [CD-ROM]*; JCPDS-ICDD: Newtown Square, PA, **2001**; pp 37−931.
30. Dieting, T. J.; Verble, J. L. Interlayer Bonding and the Lattice Vibrations of β-GaSe. *Phys. Rev. B 5* **1972**, 1473.
31. Xia, F.; Thomas, M.; Lin, Y.; Valdes-Garcia, A.; Avouris, P. Ultrafast Graphene Photodetector. *Nat. Nanotechnol.* **2009**, *4*, 839.
32. Mak, K. F.; Lee, C.; Hone, J.; Shan, J.; Heinz, T. F. Atomically Thin MoS_2: A New Direct-gap Semiconductor. *Phys. Rev. Lett.* **2010**, *105*, 136805.
33. Liu, S.; Wei, Z.; Cao, Y.; Gan, L.; Wang, Z. X.; Xu, W.; Guo, X. F.; Zhu, D. B. Ultrasensitive Water-Processed Monolayer Photodetectors. *Chem. Sci* **2011**, *2*, 796–802.